A Preliminary Study on Uncertainty of NB-IoT Measurements in Reverberation Chambers

Anouk Hubrechsen[1,2], Vincent T. Neylon[2], Kate A. Remley[2], Robert D. Jones[2], Robert D. Horansky[2], and Laurens A. Bronckers[1]

[1] Eindhoven University of Technology, Department of Electrical Engineering, Eindhoven, The Netherlands
[2] National Institute of Standards and Technology, Boulder, CO, USA

Abstract—New protocols related to internet-of-things applications may introduce previously unnoticed measurement effects due to the narrowband nature of these protocols. Such technologies also require less loading to meet the coherence bandwidth conditions, which may lead to higher variations accross the channel. This can cause a need to take additional components into account in the assessment of uncertainty. In this work, we present a preliminary study on uncertainties of NB-IoT measurements in reverberation chambers. We show a need to account for both the number of mode-stirring samples and the lack of spatial uniformity in the uncertainty analysis, where the latter generally dominates for wireless testing. We provide preliminary results for the uncertainty including both effects. We introduce a hypothesis for the effects of loading on the uncertainty, introducing that there may be an optimal loading point to minimize uncertainty, where we describe that this decision may not depend only on coherence bandwidth, but also on the number of significant modes.

Index Terms—CAT-M1, Cellular Telecommunications, Chamber transfer function, Internet of Things, Mode distribution, NB-IoT, Reverberation chamber, Uncertainty, Wireless System

I. INTRODUCTION

The use of internet-of-things (IoT) or machine-to-machine (M2M) applications is gaining popularity to meet demands such as ubiquitous coverage, increased reconfigurability, and mobility, that are required for 5G and beyond [1], [2]. These devices will largely work in the lower 5G, or sub-6 GHz, bands and will be using protocols such as the narrowband IoT (NB-IoT) and CAT-M1 (or LTE-M) protocols [1], [2].

The performance of these cellular devices is often studied over-the-air (OTA) by metrics such as Total Isotropic Sensitivity (TIS) and Total Radiated Power (TRP) [3]. These can be carried out either in an anechoic chamber (AC) or a reverberation chamber (RC). An RC is a large metal cavity, with one or more mode-stirring mechanisms to produce, on average, a uniform distribution of the fields, and can often produce faster, lower-cost, or more flexibly configurable measurements than an AC [4]. This makes an RC an excellent candidate for testing IoT devices.

RCs have been researched extensively and were shown to be suitable for TIS measurements on earlier-generation protocols, such as WCDMA (5 MHz channel bandwidth). However, for NB-IoT we expect additional challenges due to the narrowband nature of this protocol (180 kHz channel bandwidth). Traditionally, to provide accurate results, a wideband RC reference
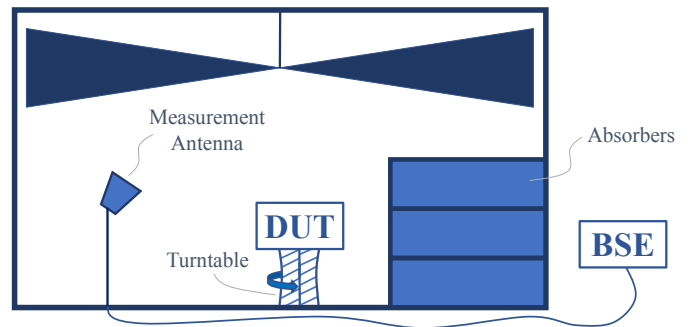
Fig. 1. Illustration of the RC setup for TIS, including a turntable for position stirring, which is needed in loaded chamber measurements.

measurement is averaged over frequency in post processing to match the bandwidth of the modulated signal. Such frequency averaging has the added benefit of smoothing the frequency response. When averaging the frequency response over a narrow bandwidth, peaks and nulls in the RC's frequency response for the mode-stirring samples may increase uncertainty, as we will show.

Earlier research has extensively studied uncertainty effects in loaded RCs for wireless-device testing [5]–[7]. For the first time, we provide a preliminary study where we show a need to incorporate both the uncertainty due to the number of mode-stirring samples *within* a data set and the uncertainty due to a lack of spatial uniformity, captured *between* data sets. We introduce a hypothesis for the effects of loading on the uncertainties. In Section II we explain the process for TIS measurements in RCs. In Section III, we provide the methodology and experimental results, where we incorporated the *within* uncertainty. In Section IV, we introduce a hypothesis support the results. The work is concluded in Section V.

II. TIS MEASUREMENT

TIS is a measure of the minimum received power that a device can accept without incurring an unacceptable throughput for a certain protocol. An illustration of a typical RC setup for a TIS measurement is shown in Fig. 1. A wireless link is set up between a base-station emulator (BSE) and a device under test (DUT), where the BSE transmits a signal at decreasing power levels at the downlink frequency, and measures the DUT's

reported throughput at the uplink frequency. TIS is defined as the minimum power incident on a DUT where the throughput drops below a certain percentage. For the NB-IoT protocol, a throughput of 95 % is used. We measure the BSE power for a high value of starting power and as long as the throughput is 95 % or higher [8], we step the power down until the throughput drops below 95 % to obtain a minimum power for each mode-stirring sample. This process is repeated for every sample in the mode-stirring sequence, and then averaged over all mode-stirring samples to obtain TIS [8].

Usually, we need to load the chamber by adding RF absorbers to flatten the RC's frequency response and to keep the communication link between the BSE and the DUT while measuring TIS. This is due to the fact that, in an unloaded chamber, the frequency selectivity is usually too high for the DUT's equalizers. This increases frequency correlation and reduces spatial uniformity, which may increase uncertainty if not compensated for using position stirring with, for example, a turntable as shown in Fig. 1 [5]. The amount of loading necessary can be determined using the coherence bandwidth (CBW), defined by the average bandwidth over which the frequency samples have a minimum specified level of correlation [9]. In general, the CBW needs to be wider than the channel bandwidth to maintain the link [8].

In the CTIA Test Plan for Large-Form-Factor IoT Devices [8], TIS is calculated by

$$P_{\text{TIS}} = G_{\text{ref}} \eta_{\text{meas}}^{\text{tot}} G_{\text{cable}} (\langle \frac{1}{P_{\text{BSE}}} \rangle_M)^{-1}, \tag{1}$$

where P_{TIS} is the total isotropic sensitivity in W and $\eta_{\text{meas}}^{\text{tot}}$ the total efficiency of the measurement antenna. G_{cable} is the cable loss between the measurement antenna and the BSE, $P_{\text{BSE}(m)}$ is the minimum received power measured by the BSE at the threshold throughput in W for mode-stirring sample m, $\langle \cdot \rangle_M$ is an ensemble average over the total number of mode-stirring samples M and G_{ref} is the chamber transfer function given by

$$G_{\text{ref}} = \frac{\langle \langle |S_{21}|^2 \rangle_M \rangle_F}{\eta_{\text{meas}}^{\text{tot}} \eta_{\text{ref}}^{\text{tot}}}, \tag{2}$$

where $\eta_{\text{ref}}^{\text{tot}}$ is the total efficiency of the reference antenna and $\langle \cdot \rangle_F$ is an ensemble average over F frequencies across the channel bandwidth. According to the standard [8], G_{ref} is used in the assessment of uncertainty, through the standard deviation of the measurement over several independent realizations of the mode-stirring sequence, defined as the *between* uncertainty. G_{ref} needs to be frequency averaged over the same bandwidth as the DUT channel being measured. However, since the channel bandwidth for NB-IoT is much narrower than previously used protocols, this will result in less frequency averaging so we may expect uncertainty to increase, as we show next.

III. EXPERIMENTAL RESULTS

In this section, we first present our measurement setup and the methods we used for estimating uncertainty. Then, we show preliminary experimental results on uncertainty.
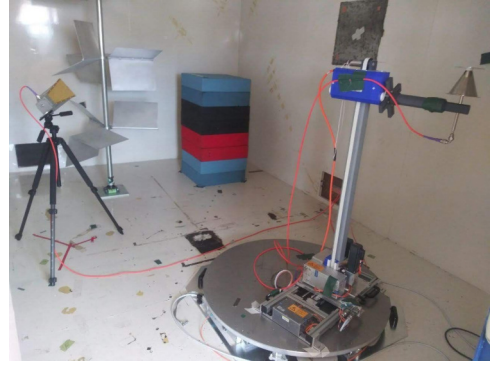
Fig. 2. RC setup to measure G_{ref} for eight absorbers. The chamber contains one vertical paddle for mode stirring, a turntable with height translation for position stirring, and automated polarization stirring.

TABLE I
MODE-STIRRING SEQUENCE FOR EACH INDEPENDENT REALIZATION (IR)

| IR | Height | Pol | Paddle angles | | Turntable |
			Angles	Offset	Angles
1-3	0.3 m	0°	8	0°, 15°, 30°	15
4-6	0.3 m	90°	8	0°, 15°, 30°	15
7-9	1.3 m	0°	8	0°, 15°, 30°	15
10-12	1.3 m	90°	8	0°, 15°, 30°	15

A. Experiment Setup

Measurements were carried out in a 4.6 m x 3.1 m x 2.8 m RC at the National Institute of Standards and Technology (NIST), as shown in Fig. 2, which has one paddle as a mode-stirring mechanism, a turntable and height translation for position stirring, and automated polarization stirring. From all mode-stirring samples, we acquired 12 independent realizations ($N_B = 12$), each containing 120 mode-stirring samples ($N_W = 120$) *within* the stirring sequence obtained from 8 paddle and 15 turntable angles with 45° and 24° angle spacing, respectively, as shown in Table I. We state that they are independent realizations based on an application of cross-correlation techniques that verified independence to within a specified threshold of 0.3 [8]. A vector network analyzer (VNA) was used, with an IF BW setting of 1 kHz, a source power of -8 dBm and a 1 kHz frequency spacing over 3 different frequency bands of 10 MHz, centered at 1993 MHz, 1995 MHz and 1999 MHz in the Cellular NB-IoT Band 2. In post processing, we chose multiple frequency averaging bandwidths to observe the effect of a narrow averaging bandwidth across frequency. We also chose two absorber cases, one with two RF absorbers (CBW = 1.5 MHz) and one with eight (CBW = 3.3 MHz), where the CBW was calculated with a threshold of 0.5. We used two low-loss broadband antennas

TABLE II
PERCENTAGE OF *between* SIGNIFICANCE IN THE FREQUENCY BAND

	180 kHz	1.2 MHz	2.0 MHz
2 Abs. (CBW ≈ 1.5 MHz)	8 %	15 %	28 %
8 Abs. (CBW ≈ 3.3 MHz)	31 %	39 %	53 %
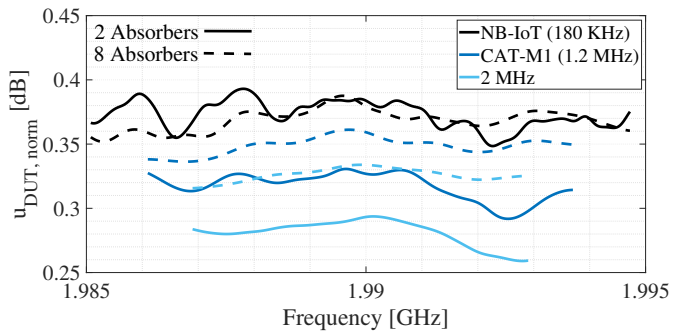
Fig. 3. Uncertainty of the DUT for two (CBW ≈ 1.5 MHz) and eight absorbers (CBW ≈ 3.3 MHz), calculated using the formulation where *within* uncertainties are dominant, for three different averaging bandwidths.

for the measurement, where the calibration reference plane was brought up to the connectors of the antennas using an N-type electronic calibration module. The measurement setup with eight absorbers is shown in Fig. 2.

B. Significance Test for Uncertainty

We perform a significance test as described in detail in [6] to determine if only the *between* uncertainty is significant, as is dictated by the current standard [8] or if the *within* uncertainty, defined by the variation due to the number of samples *within* an independent realization, should be taken into account as well, as different formulations are used depending on the outcome. As shown in Table II for the higher end of Band 2, the percentage of the frequency band where *between* uncertainties are significant increases for higher-loading cases, due to a reduced spatial uniformity. However, for both NB-IoT and CAT-M1 the *between* uncertainties are not significant for the majority of the frequency band, so the *within* component should be taken into account as well in the uncertainty (similar results were observed for the other two bands). This shows a need to reassess current uncertainty methods to be applicable to NB-IoT, which will be discussed more extensively in future publications. The formulation used in this work (taking *within* uncertainty into account as well) to determine the uncertainty of the DUT is given by [6]

$$u_{\text{DUT}}^2 = \frac{1}{N_W(N_B N_W - 1)} \sum_{i=1}^{N_W} \sum_{j=1}^{N_B} (G_R(w_i, b_j) - \hat{G}_{\text{Ref}})^2. \quad (3)$$

Next, we show results using this formulation. Note that a similar effect, where the dominant source of uncertainty changes with the specific chamber configuration, was also observed in [5], [6], but with less focus on *within* uncertainties.

C. Experiment Results

Fig. 3 shows the normalized u_{DUT} for loading cases with two and eight absorbers, averaged over various channel bandwidths. For the sake of brevity, we only show the higher-end of Band 2, but similar results were observed for the mid- and lower-end. In the current CTIA Large-Form-Factor IoT Device Test Plan [8], the user selects the highest value of u_{DUT}, computed over all frequencies within the band of interest, to find uncertainty, since, as shown in Fig. 3, uncertainty estimates can change over frequency. There are two main findings in these results. First, the maximum uncertainty is similar for both absorber cases, while, generally, uncertainty increases for increased loading [9]. Second, an increased averaging bandwidth reduces the uncertainty more in the two-absorber case, as compared to the eight-absorber case. Both effects are generally not observed in RC measurements with a wider averaging bandwidth, although for wider bandwidths, the *between* uncertainty often dominates. Next, we introduce a hypothesis for these effects. Note that this is a preliminary study so other explanations may be valid as well. Measurements over multiple bands and absorber cases in different chambers should be performed, and compared to a TIS measurement, to form definite conclusions.

IV. MODE DISTRIBUTION AND UNCERTAINTY

In this section, we introduce a possible explanation for the results, linking the amount of loading to changes in *within* and *between* uncertainties.

In an unloaded chamber, each mode is expected to be very narrowband compared to the channel bandwidth, as shown for an ideal chamber in [10]. When we load the chamber, these individual modes become wider, and, therefore, the frequency response flattens, increasing the CBW. This is illustrated in Fig. 4 (note that we normalized the maximums to illustrate a concept, it is not an illustration of the actual modes in our chamber). Considering that the NB-IoT protocol has a maximum channel bandwidth of 180 kHz, and that the CBW of an unloaded chamber is often wider than 180 kHz [9], it should be possible to perform the measurement with no loading. In wider-band measurements, this generally reduces *between* uncertainty, due to a higher spatial uniformity. However, earlier work on NB-IoT TIS measurements did use chamber loading [11], but no reason was stated. Besides that, the results show a similar maximum *within* uncertainty for
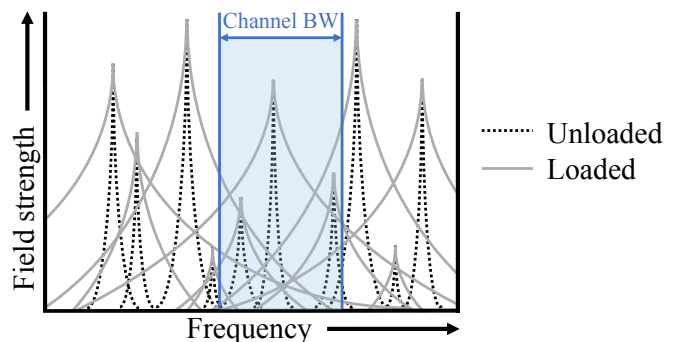
Fig. 4. Illustration of the mode distribution in a loaded and an unloaded RC. The modes spread more across frequency in the channel bandwidth for higher loading cases. Even though these are all correlated within the CBW, sharp peaks and nulls are flattened by the addition of more significant modes.

both loading cases. Therefore, a need arises to assess the effects of chamber loading on the *within* uncertainty together with the question if some chamber loading may be preferable, even in cases where the CBW is already wider than the channel bandwidth.

We expect the following effects to influence *within* uncertainty in cases when the channel bandwidth is narrow:

- A higher averaging bandwidth reduces the amount of peaks and nulls in the frequency response, reducing *within* uncertainty. Therefore, a user may require more mode-stirring samples for narrowband measurements. This effect can be observed in both CBW cases in Fig. 3.
- Fewer significant modes (modes with a significant contribution to the measured S-parameter at a given frequency [12]) may be included in each channel for narrowband measurements. This may result in higher peaks and nulls in the frequency response and an increased *within* uncertainty (this is likely related to the previous point).
- If chamber loading is increased, the frequency response flattens, and the amount of significant modes may increase (contributions from modes that were mostly outside of the channel bandwidth in an unloaded case may occur in-band for a loaded case) [12], [13], as illustrated in Fig. 4. Due to the presence of more significant modes within the band, the *within* uncertainty may decrease, even though all the frequency samples in the channel bandwidth are more correlated due to increased loading. Note that this example only holds for one mode-stirring sample, but consequently could affect the average of all measurements as well. This is a possible explanation on why increased frequency averaging had less of a reduction in uncertainty in the 8-absorber case, since *within* differences may have been reduced already by loading, reducing the effect of additional frequency averaging.

Combining these three statements on the effect of loading on the uncertainty as defined in (3), one could state that there may be an optimal-loading point for narrowband TIS measurements, as illustrated in Fig. 5. This point would be a trade-off, where the frequency response is flattened sufficiently such that peaks and nulls are averaged out, but the chamber is not loaded to a point where the spatial uniformity decreases in such way that *between* differences become significant, given a significant amount of position stirring. Note that a similar
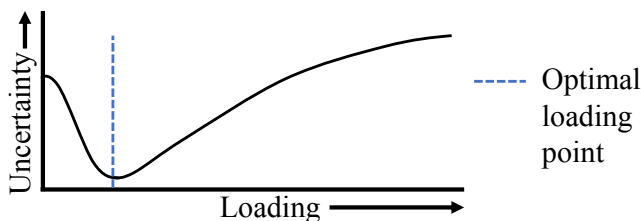
Fig. 5. Illustration of the expected effect on uncertainty by an increase in chamber loading. Uncertainty first decreases because there are more significant modes in the channel bandwidth, but increases for higher loading due to high correlations.

effect was observed in [13] for small added loss, where loss resulted in a benefit to convergence to an overmoded (sufficient significant modes) condition. The proposed approach could be more extensive than the current approach where one defines the amount of loading only by use of the CBW, but as stated earlier, a more extensive study should be performed to form definitive conclusions.

V. CONCLUSION

In this paper, we have shown that current methods in the assessment of uncertainty for TIS measurements of IoT devices may need to be reassessed due to the narrowband nature of the NB-IoT protocol. We introduced a hypothesis that links the effects of loading on the mode-distribution to a reduced uncertainty, taking both variations *between* and *within* the data sets into account, leading to a possible optimal-loading point. However, more extensive measurements should be performed and compared to the uncertainty of a full TIS measurement to form definite conclusions. Future publications will contain a more extensive assessment of the uncertainty in (3), and will provide more elaborate results for u_{DUT}^2 and TIS.

REFERENCES

[1] GSMA, "Mobile IoT in the 5G future: NB-IoT and LTE-M in the context of 5G," Apr 2018.

[2] 3GPP TS 36.101, "Evolved universal terrestrial radio access (E-UTRA); user equipment (UE) radio transmission and reception (release 16)," Dec 2019.

[3] R. D. Horansky, T. B. Meurs, M. V. North, C. Wang, M. G. Becker, and K. A. Remley, "Statistical considerations for total isotropic sensitivity of wireless devices measured in reverberation chambers," in *2018 International Symposium on Electromagnetic Compatibility (EMC EUROPE)*, Aug 2018, pp. 398–403.

[4] R. D. Horansky and K. A. Remley, "Flexibility in over-the-air testing of receiver sensitivity with reverberation chambers," *IET Microwaves, Antennas Propagation*, vol. 13, no. 15, pp. 2590–2597, 2019.

[5] M. G. Becker, M. Frey, S. Streett, K. A. Remley, R. D. Horansky, and D. Senic, "Correlation-based uncertainty in loaded reverberation chambers," *IEEE Transactions on Antennas and Propagation*, vol. 66, no. 10, pp. 5453–5463, Oct 2018.

[6] K. A. Remley, C. J. Wang, D. F. Williams, J. J. aan den Toorn, and C. L. Holloway, "A significance test for reverberation-chamber measurement uncertainty in total radiated power of wireless devices," *IEEE Transactions on Electromagnetic Compatibility*, vol. 58, no. 1, pp. 207–219, Feb 2016.

[7] X. Chen, P. Kildal, and S. Lai, "Estimation of average rician k-factor and average mode bandwidth in loaded reverberation chamber," *IEEE Antennas and Wireless Propagation Letters*, vol. 10, pp. 1437–1440, 2011.

[8] CTIA Certification, "Test plan for wireless large-form-factor device over-the-air performance, version 1.2.1," Feb 2019.

[9] K. A. Remley, J. Dortmans, C. Weldon, R. D. Horansky, T. B. Meurs, C. Wang, D. F. Williams, C. L. Holloway, and P. F. Wilson, "Configuring and verifying reverberation chambers for testing cellular wireless devices," *IEEE Transactions on Electromagnetic Compatibility*, vol. 58, no. 3, pp. 661–672, June 2016.

[10] P. Besnier and B. Démoulin, *Electromagnetic Reverberation Chambers*, 2011, vol. 1.

[11] J. Luo, E. Mendivil, and M. Christopher, "Over-the-air performance evaluation of NB-IoT in reverberation chamber and anechoic chamber," in *2018 AMTA Proceedings*, Nov 2018, pp. 1–3.

[12] F. Monsef and A. Cozza, "Average number of significant modes excited in a mode-stirred reverberation chamber," *IEEE Transactions on Electromagnetic Compatibility*, vol. 56, no. 2, pp. 259–265, 2014.

[13] A. Cozza, "The role of losses in the definition of the overmoded condition for reverberation chambers and their statistics," *IEEE Transactions on Electromagnetic Compatibility*, vol. 53, no. 2, pp. 296–307, 2011.